Stability of coflowing capillary jets under nonaxisymmetric perturbations

J. M. Montanero*
Departamento de Ingeniería Mecánica, Energética y de los Materiales, Universidad de Extremadura, E-06071 Badajoz, Spain

A. M. Gañán-Calvo
Departamento de Ingeniería Aeroespacial y Mecánica de Fluidos, Universidad de Sevilla, E-41092 Sevilla, Spain

(Received 2 January 2008; published 3 April 2008)

In this paper, linear hydrodynamic stability analysis is used to study the response of a capillary jet and a coflowing fluid to both axisymmetric and nonaxisymmetric perturbations. The temporal analysis revealed that nonaxisymmetric perturbations were damped (or overdamped) within the region of parameter space explored, which involved equal velocities for the jet and focusing fluid. It is explained how an extension to a spatiotemporal analysis implies that those perturbations can yield no transition from convective (jetting) to absolute (whipping) instability for that parameter region. This result provides a theoretical explanation for the absence of that kind of transition in most experimental results in the literature.

DOI: 10.1103/PhysRevE.77.046301 PACS number(s): 47.55.D−, 47.20.Dr, 47.55.db

Understanding the instability mechanisms that lead to the breakup of liquid (gas) jets into droplets (bubbles) is of great interest not only in fluid mechanics, but also in the fields of industry, medicine, biotechnology, etc. The hydrodynamic stability theory of spatially developing flows has proven to be a useful tool to predict and explain the transition from stable to unstable flow or between different types of instability [1,2]. There are two main prerequisites for the results of that theory to be reliable: the model must include all significant effects (viscosity, inertia, interfacial tension forces,…), and the basic flow around which infinitesimal perturbations are considered must be realistic. In this context, the jetting-dripping transition of a liquid [4–6] or gas [7] jet has been successfully linked to the convective-absolute instability transition for axisymmetric ($m=0$) perturbations. Also, whipping instabilities (violent lateral motion) have been observed experimentally when, for instance, a jet composed of a highly viscous molten liquid (e.g., a molten glass) is used to form fibers [8]. Determining the conditions under which whipping instabilities appear is an interesting problem both in terms of fundamental physics and technologically. By drawing an analogy with the explanation of the jetting-dripping transition, one may assume that the appearance of whipping instabilities could be explained in terms of a convective-absolute instability transition for nonaxisymmetric ($m=1$) modes. To the best of our knowledge, this possibility has not as yet been explored.

Practical problems where the present study is applicable, among others, are the simple coflow arrangement of Suryo and Basaran [3] or the double flow focusing arrangement recently proposed to produce submicrometer liquid jets by purely hydrodynamic means [9]. Both involve a liquid stream which envelopes an inner thin capillary jet of a second liquid immiscible with the former and moving with its same velocity. In the second arrangement [9], the enveloping liquid stream is in turn focused by a third current of a gas forced through a small round orifice. The basic flow in the compound jet issuing from the manifold capillary is characterized by a transversal velocity and pressure nearly constant once the jet exits through the discharge orifice. The external layer of the coaxial jet can be considered as infinite in terms of the inner jet radius. Thus the basic flow to be considered in the stability analysis is the same for the two examples referred to above. The stability of the innermost capillary jet was found to be crucial to ensure its formation down to extremely small sizes, as shown experimentally and numerically. An analysis of the convective-absolute instability transition for axisymmetric ($m=0$) perturbations in the limit of small Reynolds number showed that those perturbations are convected downstream provided that the velocity exceeds a certain threshold. This threshold depends on the viscosities and interfacial tension but is independent of the jet radius (unconditional jetting). This theoretical prediction was confirmed by experiments in [9]. The present paper aims at describing the growth of nonaxisymmetric ($m=1,2$) perturbations which could potentially yield whipping instabilities of the basic flow characterizing the proposed double flow focusing configuration, or any other similar arrangement. To this end, a three-dimensional hydrodynamic analysis is performed considering the viscosity and inertia of both the inner jet and coflowing stream. As will be shown, a temporal analysis allows one to conclude that nonaxisymmetric modes cannot lead to a global instability (whipping) at least within the parameter region explored in our study.

Consider the velocity $\mathbf{v}(\mathbf{r},t)\equiv[u(\mathbf{r},t),v(\mathbf{r},t),w(\mathbf{r},t)]$ and pressure $p(\mathbf{r},t)$ fields, and the interface position $f(\theta,z,t)$. In what follows, we shall make all the variables dimensionless using R, V, R/V, and $\rho_1 V^2$ as the characteristic length, velocity, time, and pressure, respectively, where R, V, and ρ_1 are the inner jet radius, velocity, and density, respectively. Assume that the inner jet and the coflowing fluid move with the same velocity V [9]. Using a Lagrangian frame of reference solidly moving with both fluids, we propose the following dependence for the hydrodynamic fields and the interface position:

$$\mathbf{v}_j(\mathbf{r},t)=\varepsilon\{U_j(r),V_j(r),W_j(r)\}e^{i(m\theta+kz-\omega t)}+\text{c.c.}, \quad (1a)$$

*jmm@unex.es

$$p_j(\mathbf{r},t) - \frac{\delta_{j1}}{\mathrm{We}} = \varepsilon P_j(r) e^{i(m\theta+kz-\omega t)} + \text{c.c.}, \tag{1b}$$

$$f(\theta,z,t) - 1 = \varepsilon F e^{i(m\theta+kz-\omega t)} + \text{c.c.}, \tag{1c}$$

where $j=1$ and 2 stand for the inner jet and coflowing fluid, respectively, m is the azimuthal wave number, $k=k_r+ik_i$ the axial wave number, $\omega=\omega_r+i\omega_i$ the frequency, $\mathrm{We}=\rho_1 V^2 R/\sigma$ the Weber number, σ the interfacial tension, and δ_{ij} the Kronecker delta.

If one introduces Eq. (1a)–(1c) into the Navier-Stokes equations and neglects terms in ε^2, one gets

$$U_j' + U_j/r + imV_j/r + ikW_j = 0, \tag{2a}$$

$$-\alpha^{\delta_{j2}} i\omega U_j + P_j' = \frac{\beta^{\delta_{j2}}}{\mathrm{Re}}[U_j'' + U_j'/r - (m^2+1)U_j/r^2 - k^2 U_j - 2imV_j/r^2], \tag{2b}$$

$$-\alpha^{\delta_{j2}} i\omega V_j + imP_j/r = \frac{\beta^{\delta_{j2}}}{\mathrm{Re}}[V_j'' + V_j'/r - (m^2+1)V_j/r^2 - k^2 V_j + 2imU_j/r^2], \tag{2c}$$

$$-\alpha^{\delta_{j2}} i\omega W_j + ikP_j = \frac{\beta^{\delta_{j2}}}{\mathrm{Re}}(W_j'' + W_j'/r - m^2 W_j/r^2 - k^2 W_j), \tag{2d}$$

where $\alpha \equiv \rho_2/\rho_1$, $\beta \equiv \mu_2/\mu_1$, and $\mathrm{Re}=\rho_1 VR/\mu_1$ is the Reynolds number. The general solution to Eq. (2a)–(2d), verifying the regularity conditions

$$U_1(0) = V_1(0) = W_1'(0) = 0 \quad \text{for } m=0, \tag{3a}$$

$$U_1(0) + iV_1(0) = W_1(0) = 0 \quad \text{for } m=1, \tag{3b}$$

$$U_1(0) = V_1(0) = W_1(0) = 0 \quad \text{for } m \geq 2, \tag{3c}$$

$$U_2 = V_2 = W_2 = P_2 = \text{bounded at } r \to \infty, \tag{3d}$$

can be written as

$$U_j(r) = ic_{j1}\Theta_m'(kr) + ic_{j2}\Theta_m'(k_j r) + imc_{j3}\frac{\Theta_m(k_j r)}{k_j r}, \tag{4a}$$

$$V_j(r) = -mc_{j1}\frac{\Theta_m(kr)}{kr} - mc_{j2}\frac{\Theta_m(k_j r)}{k_j r} - c_{j3}\Theta_m'(k_j r), \tag{4b}$$

$$W_j(r) = -c_{j1}\Theta_m(kr) - c_{j2}k_j\frac{\Theta_m(k_j r)}{k}, \tag{4c}$$

$$P_j(r) = -\frac{\alpha^{\delta_{j2}}\omega c_{j1}}{k}\Theta_m(kr). \tag{4d}$$

Here, Θ_m is the modified Bessel function of the first kind I_m if $j=1$, and of the second kind K_m if $j=2$, $k_1 = \pm\sqrt{k^2 - i\omega\,\mathrm{Re}}$, $k_2 = \sqrt{k^2 - i\omega\,\mathrm{Re}\,\alpha/\beta}$, and $\{c_{j1}, c_{j2}, c_{j3}\}$ are six arbitrary constants. It must be noted that Eq. (4a)–(4d) is symmetric with respect to k_1, while the real part of k must be positive to satisfy Eq. (3d).

The nonslip condition $\{U_1=U_2,\ V_1=V_2,\ W_1=W_2\}$ at the interface $r=1$ yields a linear system of equations that allows one to obtain $\{c_{21}, c_{22}, c_{23}\}$ in terms of $\{c_{11}, c_{12}, c_{13}\}$. The condition of dynamical equilibrium at the interface $r=1$ for the normal and two tangential components leads to

$$P_1 - P_2 + \frac{i(1-m^2-k^2)}{\mathrm{We}\,\omega}U_1 = \frac{2}{\mathrm{Re}}(U_1' - \beta U_2'), \tag{5a}$$

$$W_1' + ikU_1 = \beta(W_2' + ikU_2), \tag{5b}$$

$$imU_1 + V_1' - V_1 = \beta(imU_2 + V_2' - V_2), \tag{5c}$$

where use has been made of the kinematic compatibility condition $F=iU_j(1)/\omega$ to eliminate F from Eq. (5a). The set of Eqs. (5a)–(5c) constitutes a linear system of equations for $\{c_{11}, c_{12}, c_{13}\}$. The solvability condition $\mathrm{Det}(\Delta_{ij})=0$, with Δ_{ij} being the 3×3 matrix associated with that system of equations, yields the dispersion relation [10]

$$S_m(k,\omega,\alpha,\beta,\mathrm{Re},\mathrm{We}) = 0. \tag{6}$$

We have verified that Eq. (6) reduces to the result obtained by Rayleigh [1] for $m=\alpha=\beta=0$, by Bauer [11] for $\alpha=\beta=0$ and $m\neq 0$, and by Funada and Joseph [12] (or, independently, by Gañán-Calvo and Riesco-Chueca [5]) for $m=0$ and $\alpha,\beta\neq 0$. It can be easily verified that Eq. (6) can be rewritten in the form

$$Q_m(k,\tilde{\omega},\alpha,\beta,\mathrm{Oh}) = 0, \tag{7}$$

where $\tilde{\omega}=\tilde{\omega}_r+i\tilde{\omega}_i \equiv \mathrm{We}^{1/2}\omega$ and $\mathrm{Oh}\equiv \mathrm{We}^{1/2}/\mathrm{Re}$ is the Ohnesorge number. This is equivalent to choosing the capillary velocity $V_c \equiv (\sigma/\rho_1 R)^{1/2}$ instead of V as the characteristic velocity, an appropriate choice when the flow is described in our Lagrangian frame of reference. It must be noted that this simplification is exclusive to the basic flow considered here, where both the inner jet and the coflowing fluid move with the same velocity V, and allows one to study its response to perturbations over a significant region of parameter space at a reasonable computational cost: in this work we have explored the modes $m=0,1$, and 2, for $0.01\leq \mathrm{Oh}\leq 10$, and $10^{-4}\leq\alpha,\beta\leq 10$. In particular, for $m=0$, we have explored $10^{-6}\leq\alpha,\ \beta\leq 1$, $10^{-7}\leq \mathrm{We}\leq 10^3$, and $10^{-7}\leq \mathrm{Re}\leq 10^6$.

Let us now calculate the growth factor $\tilde{\omega}_i$ of a perturbation with a *real* axial wave number k (temporal analysis) observed from the frame of reference moving with both fluids. Our goal is to obtain the roots of Eq. (7) in the parameter space $\{k,\tilde{\omega},\alpha,\beta,\mathrm{Oh}\}$ for different values of the azimuthal wave number m. To this end, solutions $\tilde{\omega}$ to Eq. (7) in the complex plane $(\tilde{\omega}_r,\tilde{\omega}_i)$ were found numerically for fixed values of the rest of the parameters. Because we were mainly interested in finding possible transitions from stable ($\tilde{\omega}_i<0$) to unstable ($\tilde{\omega}_i>0$) perturbations, Eq. (7) was carefully explored close to the $\tilde{\omega}_i=0$ axis, while less attention was paid to other regions of the $(\tilde{\omega}_r,\tilde{\omega}_i)$ plane. For nonsurrounded jets ($\alpha=\beta=0$), it is well-known that both axisymmetric ($m=0$) [1] and nonaxisymmetric ($m\neq 0$) [11,13] perturbations are

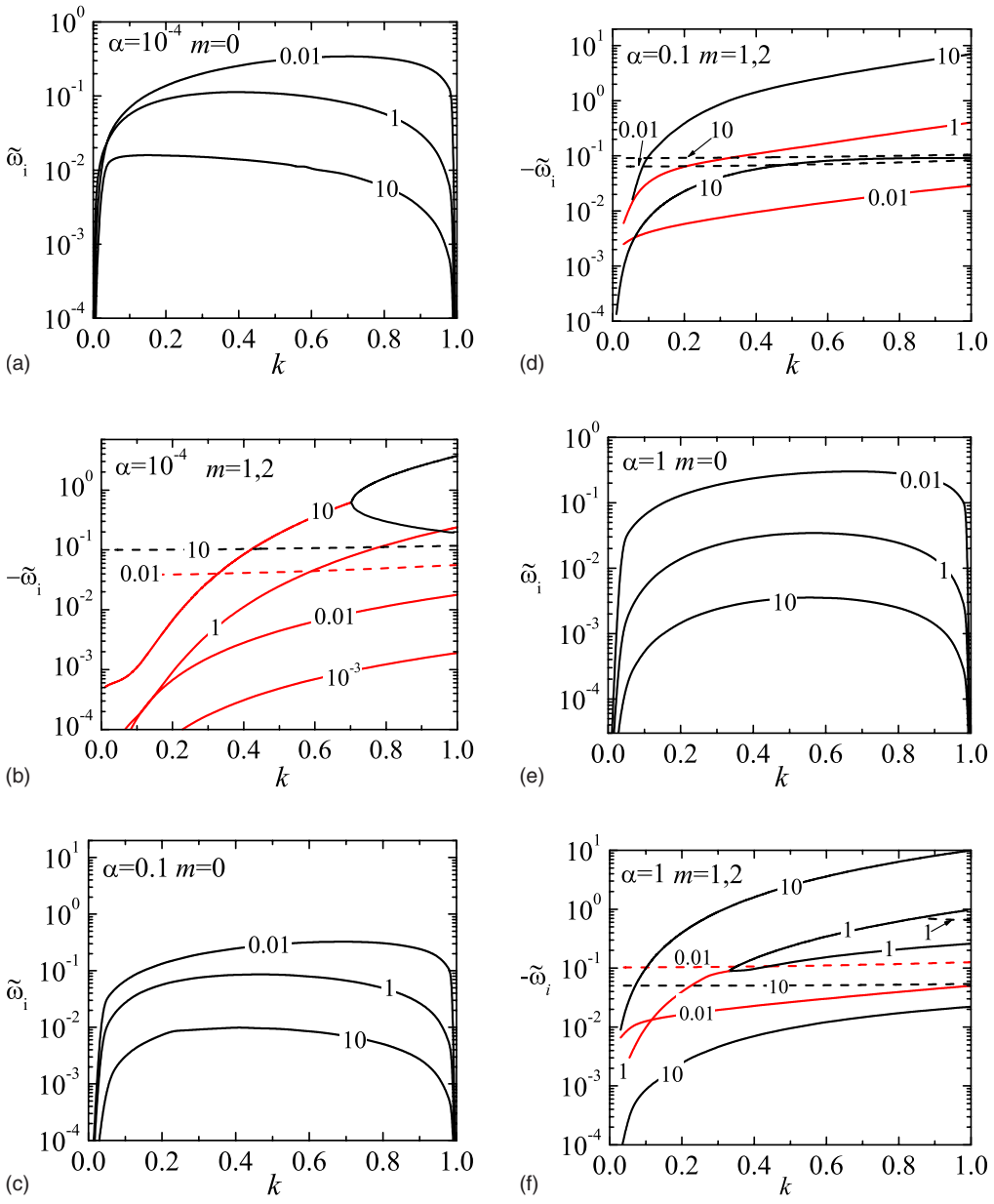

FIG. 1. (Color online) Growth factor $\tilde{\omega}_i$ as a function of k for $m=0$ (left) and $m=1,2$ (right). The solid and dashed lines in the plots on the right correspond to $m=1$ and 2, respectively. The labels on the lines indicate the value of Oh. The black curves correspond to growing ($m=0$) and overdamped ($m\neq 0$) motions, while the gray (red on-line) curves correspond to oscillatory motions.

stable for $k>1$, while for $0<k<1$ the axisymmetric perturbations are unstable and cause the breakup of the jet (column). For this reason, we compared the growth factors of focused jets for different values of m within the interval $0 \leq k \leq 1$ in the present study. Because of the large size of the parameter space, it was explored partially by restricting ourselves to the cases $m=0$, 1, and 2. The range of Oh values considered contained those considered in previous experiments [5]. The roots of Eq. (7) were found by means of the Newton-Raphson method using as an initial guess that obtained from a linear extrapolation of the two previous solutions. To improve the accuracy of the procedure, the function Q_m was normalized by dividing it by its value at the initial guess. An additional graphical analysis was eventually required to discard spurious roots.

Figures 1–4 summarize the results of our analysis. They show the growth factor in terms of the capillary time $t_c \equiv (\rho_1 R^3/\sigma)^{1/2}$. The results for fluids with the same kinematic viscosity ($\alpha=\beta$) and $\alpha \leq 1$ are plotted in Fig. 1. For $m=0$, nonoscillatory ($\tilde{\omega}_r=0$) perturbations of growing amplitude ($\tilde{\omega}_i>0$) were observed, while damped ($\tilde{\omega}_r\neq 0$ and $\tilde{\omega}_i<0$) and overdamped ($\tilde{\omega}_r=0$ and $\tilde{\omega}_i<0$) oscillations were found for $m\neq 0$. The black curves correspond to growing ($m=0$) and overdamped ($m\neq 0$) motions, while the gray (red online) curves correspond to oscillatory motions. The stabilizing effect of the viscosity can be appreciated: the growth rate decreases with Oh for the unstable axisymmetric perturbations, while the damping rate increases with Oh for the stable nonaxisymmetric ones. The bifurcations observed for $\alpha=10^{-4}$ and Oh=10 at $k\simeq 0.7$, and for $\alpha=\mathrm{Oh}=1$ at $k\simeq 0.3$, in

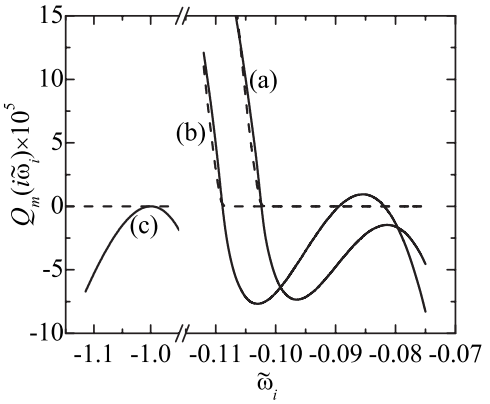

FIG. 2. Real (dashed lines) and imaginary (solid lines) parts of $Q_m(k, i\tilde{\omega}_i, \alpha, \beta, \mathrm{Oh})$ as a function of $\tilde{\omega}_i$ for $\alpha=\beta=m=\mathrm{Oh}=1$ and $k=0.32$ (a) and 0.33 (b), and for $\alpha=\beta=10^{-4}$, $m=2$, and $\mathrm{Oh}=k=1$ (c).

both cases for $m=1$, correspond to transitions from damped to overdamped oscillations, for which Eq. (7) admits two solutions for each value of k. To illustrate this point, Fig. 2 shows the real and imaginary parts of Q_m along the imaginary axis for $\alpha=\mathrm{Oh}=m=1$. A damped oscillation is obtained for $k=0.32$, and thus the root of Eq. (7) is not located on the imaginary axis. On the contrary, for $k=0.33$ one finds two roots $\tilde{\omega}_i=-0.081\,82$ and $-0.089\,43$ that correspond to the

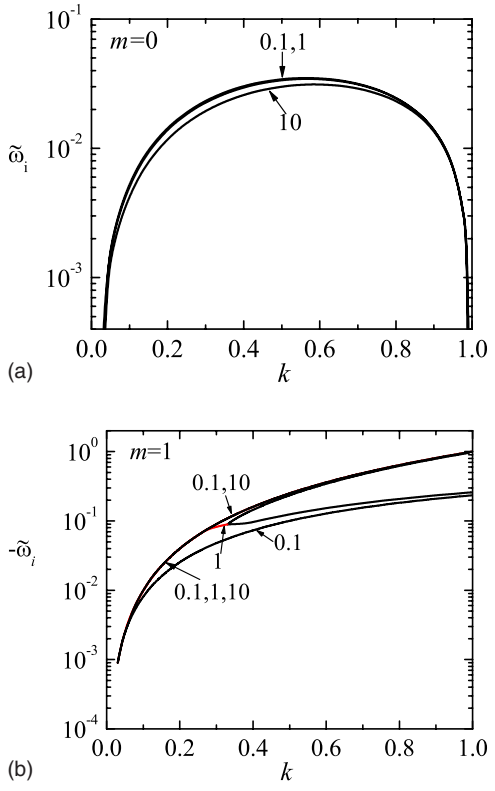

FIG. 3. (Color online) Growth factor $\tilde{\omega}_i$ as a function of k for $\beta=\mathrm{Oh}=1$ and for $m=0$ (a) and $m=1$ (b). The labels on the lines indicate the value of α. The black curves correspond to growing ($m=0$) and overdamped ($m=1$) motions, while the gray (red online) curves correspond to oscillatory motions.

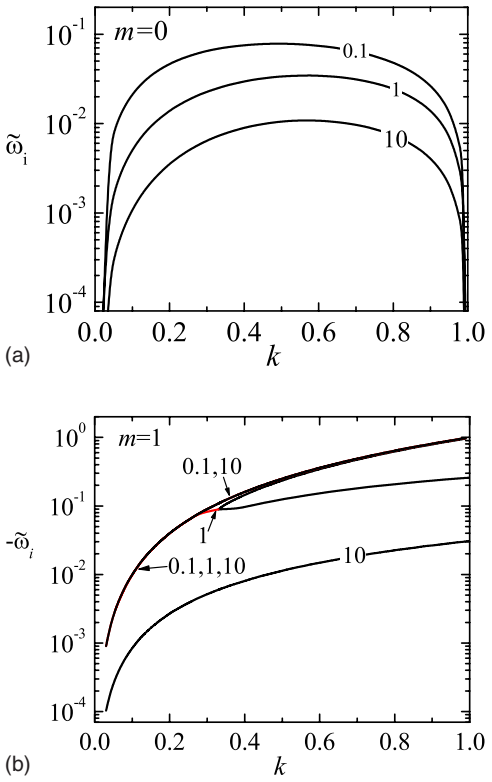

FIG. 4. (Color online) Growth factor $\tilde{\omega}_i$ as a function of k for $\alpha=\mathrm{Oh}=1$ and for $m=0$ (a) and $m=1$ (b). The labels on the lines indicate the value of β. The black curves correspond to growing ($m=0$) and overdamped ($m=1$) motions, while the gray (red online) curves correspond to oscillatory motions.

dominant and subdominant solutions, respectively. The curves (a) and (b) apparently vanish at $\tilde{\omega}_i=-0.102$ and -0.109, respectively, but these values do not correspond to true solutions of the dispersion relation within the accuracy of our numerical calculations. Dominant and subdominant solutions were also obtained for $\alpha=0.1$ and 1, $m=1$, and $\mathrm{Oh}=10$ in the interval $0\leq k\leq 1$. We found both oscillatory and overdamped motions with $m=2$ as well. In the latter case, only the dominant motions are plotted in the figure. We only obtained spurious roots for $m=2$, $\mathrm{Oh}=1$, and $\alpha=10^{-4}$ and 0.1 within the region of the ω plane explored. This result is also illustrated in Fig. 2. The curve (c) apparently vanishes at $\tilde{\omega}_i=-1$, but it does not seem to correspond to a true solution of the dispersion relation within the accuracy of our numerical calculations.

Figure 3 shows the influence of the density ratio α on the growth factor $\tilde{\omega}_i$ for fluids with the same viscosity ($\beta=1$). For $m=0$, growing motions ($\tilde{\omega}_i>0$) were obtained, the influence of α on $\tilde{\omega}_i$ being small. For $m=1$, all the perturbations were stable and the density ratio affected the nature of the motion. Damped oscillations with very small frequencies ($|\tilde{\omega}_i|\ll 1$) were observed for $\alpha=10$, while (dominant and subdominant) overdamped motions ($\tilde{\omega}_i=0$) were obtained for $\alpha=0.1$. As mentioned above, the solution for the intermediate value $\alpha=1$ exhibits a bifurcation at $k\simeq 0.3$ which corresponds to a transition from oscillatory ($k\lesssim 0.3$) to overdamped ($k\gtrsim 0.3$) motions. The growth factors corresponding

to the oscillatory and subdominant overdamped solutions practically coincided (for which reason the color cannot be appreciated in the plot).

Figure 4 illustrates the influence of the viscosity ratio β for liquids with the same density ($\alpha=1$). The viscosity ratio significantly affects the growth factor for $m=0$. For $m=1$, one finds a scenario similar to that of Fig. 3. In fact, the oscillatory and subdominant overdamped solutions practically coincide in both cases. This is because those solutions depend on α and β essentially through the ratio α/β in k_2, and this ratio takes the same values in both figures.

The most important conclusion drawn from the analysis of the results shown in Fig. 1 (and others not presented here) is that nonaxisymmetric perturbations possess negative growth factors within the region of parametrical space explored. The same conclusion was obtained in Refs. [11,13] for other values of k and Oh in the particular case $\alpha=\beta=0$. A natural question is whether a transition from convective (jetting) to absolute (whipping) instability for $m\neq 0$ is compatible with this scenario. To answer this question one should explore the response of the system to perturbations characterized by a *complex* axial wave number k (spatiotemporal analysis), observed by a fixed observer anchored at the nozzle. To change the frame of reference from a traveling observer to a fixed one, we just need to replace the wave frequency ω by $\omega'-k$ in the dispersion relation (6) [5]. It must be noted that the resulting dispersion relation

$$R_m(k,\omega',\alpha,\beta,\mathrm{Re},\mathrm{We})=0 \tag{8}$$

cannot be rewritten in the form (7), and so the parameter space becomes $\{k,\omega',\alpha,\beta,\mathrm{We},\mathrm{Re}\}$ in the laboratory frame of reference. The transition from convective to absolute instability occurs for values of (Re, We) for which there is at least one solution (k_0,ω_0') of the dispersion relation (8) satisfying $d\omega'/dk=0$ (zero group velocity) with $\omega_i'=0$ [2,5,7]. In addition, the spatial branches departing from that solution must originate from distinct halves of the k plane [2], which implies that there must exist at least one solution of the dispersion relation with $\omega_i'=k_i=0$.

One can find solutions of the problem formulated above for $m=0$ [5]. Figure 5(a) shows the transition curves from jetting to dripping for $\alpha=\beta=10^{-6}$, 10^{-3}, and 1. In the limit $\mathrm{Re}\to 0$, the transition takes place for critical values of the Capillary number $\mathrm{Ca}\equiv(\mu_1\mu_2)^{1/2}V/\sigma$, independently of the jet radius (unconditional jetting) [9]. In Fig. 5(b), we plot the spatial branches $k_\pm(\omega')$ for $\mathrm{Re}=0.1260$ and $\mathrm{We}=0.02101$ that originated from the solution $k_0=0.5828-0.3921i$ and $\omega_0'=0.5757$. As can be observed, the branch k_+ crosses the k_r axis at $k_r=1$ (Rayleigh stability limit), and thus the condition $\omega_i'=k_i=0$ mentioned above is verified.

The condition $\omega_i'=k_i=0$ cannot be verified for $m\neq 0$ at least within the region of parameter space considered in our temporal analysis (Fig. 1). To demonstrate this assertion, we

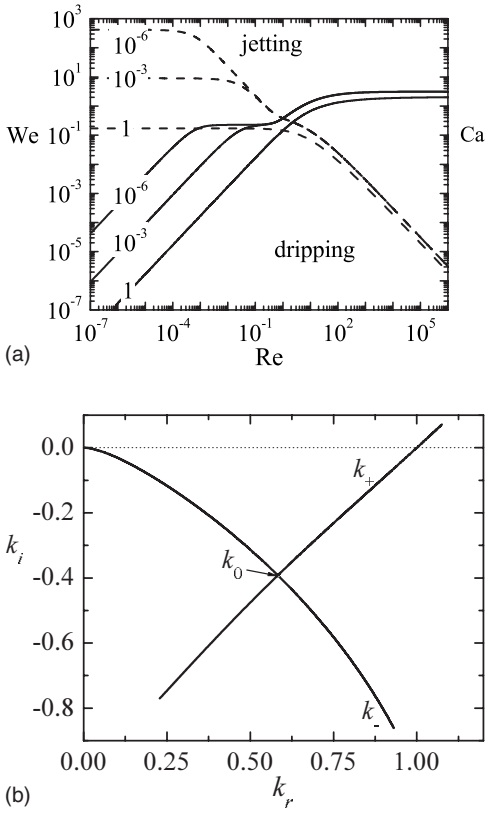

FIG. 5. (a) Transition curves for $m=0$ and $\alpha=\beta=10^{-6}$, 10^{-3}, and 1, and (b) spatial branches $k_\pm(\omega')$ for $\mathrm{Re}=0.1260$ and $\mathrm{We}=0.02101$ that originated from the solution $k_0=0.5828-0.3921i$ and $\omega_0'=0.5757$. In plot (a), the solid and dashed lines correspond to the transition curves on the (Re,We) and (Re,Ca) planes, respectively.

shall assume that there is a solution of the dispersion relation (8) with $\omega_i'=k_i=0$ for $m\neq 0$. As the solutions of Eqs. (7) and (8) are related through the equation $\tilde{\omega}=\mathrm{Re}(\omega'-k)$, there would also exist a solution of Eq. (7) with $\tilde{\omega}_i=k_i=0$, in contrast to what is shown in Fig. 1. Therefore a transition from convective to absolute instability cannot take place for $m\neq 0$.

The above result constitutes a theoretical explanation of the absence of transition from jetting to whipping in most of the experiments conducted so far. This explanation possesses, however, two main limitations. First, the basic flow around which perturbations were considered must correspond to the experimental flow. This can be assumed for the double focusing arrangement recently proposed to produce monodisperse submicrometer liquid droplets [9]; and second, our conclusions might not be valid for other choices of the experimental parameters α, β, and Oh.

Partial support from the MCYT (Spain) through Grant No. DPI2007-63559 is acknowledged.

[1] S. Chandrasekhar, *Hydrodynamic and Hydromagnetic Stability* (Oxford University Press, Oxford, England, 1961).
[2] P. Huerre and P. A. Monkewitz, Annu. Rev. Fluid Mech. **22**, 473 (1990).
[3] R. Suryo and O. A. Basaran, Phys. Fluids **18**, 082102 (2006).
[4] S. P. Lin, *Breakup of Liquid Sheets and Jets* (Cambridge University Press, Cambridge, England, 2003).
[5] A. M. Gañán-Calvo and P. Riesco-Chueca, J. Fluid Mech. **553**, 75 (2006).
[6] P. Guillot, A. Colin, A. S. Utada, and A. Ajdari, Phys. Rev. Lett. **99**, 104502 (2007).
[7] A. M. Gañán-Calvo, M. A. Herrada, and P. Garstecki, Phys. Rev. Lett. **96**, 124504 (2006).
[8] A. M. Gañán-Calvo, M. Pérez-Saborid, J. M. López-Herrera, and J. M. Gordillo, Eur. Phys. J. B **39**, 131 (2004).
[9] A. M. Gañán-Calvo, R. González-Prieto, P. Riesco-Chueca, M. A. Herrada, and M. Flores-Mosquera, Nat. Phys. **3**, 737 (2007).
[10] Because of the three-dimensional nature of the flow, the dispersion relation is considerably more complicated than in [5,7], and thus a practical explicit expression of Eq. (6) cannot be provided. A MATHEMATICA notebook containing the dispersion relation can be supplied upon request to the authors.
[11] H. F. Bauer, Z. Angew. Math. Mech. **64**, 475 (1984).
[12] T. Funada and D. D. Joseph, Int. J. Multiphase Flow **28**, 1459 (2002).
[13] D. Langbein, Microgravity Sci. Technol. **5**, 73 (1992).